Bull. Mater. Sci., Vol. 35, No. 6, November 2012, pp. 947–956. © Indian Academy of Sciences.

Structural and optical properties of Zn doped $CuInS_2$ thin films

MAHDI H SUHAIL
Department of Physics, College of Science, University of Baghdad, Iraq

MS received 19 October 2011; revised 11 January 2012

Abstract. **Copper indium sulphide (CIS) films were deposited by spray pyrolysis onto glass substrates from aqueous solutions of copper (II) sulphate, indium chloride and thiourea using compressed air as the carrier gas. The copper/indium molar ratio (Cu/In) in the solution 1(1:1) and the sulphur/copper ratio (S/Cu) was fixed at 4. Structural properties of these films were characterized. The effects of Zn (0–5%) molecular weight compared with $CuInS_2$ Source and different substrate temperatures on films properties were investigated using X-ray diffraction (XRD) and optical transmission spectra. Optical characteristics of the $CuInS_2$ films have been analysed using spectrophotometer in the wavelength range 300–1100 nm. The absorption spectra of the films showed that this compound is a direct bandgap material and gap values varied between 1·55 and 1·57 eV, depending on the substrate temperatures. Zn-doped samples have a bandgap energy of 1·55–1·95 eV. It was observed that there is an increase in optical bandgap with increasing Zn % molecular weight. The optical constants of the deposited films were obtained from the analysis of the experimentally recorded transmission and absorption spectral data. The refractive index, n and dielectric constants, ε_1 and ε_2, were also discussed and calculated as a function of investigated wavelength range and found it dependent on Zn incorporation. We found that the Zn-doped $CuInS_2$ thin films exhibit P-type conductivity and we predict that Zn species can be considered as suitable candidates for use as doped acceptors to fabricate $CuInS_2$-based solar cells. The paper presents a study concerning the influence of deposition parameters (temperature of the substrate and concentration of Zn (1–5)% from 0·16 M $ZnCl_2$) on the quality of $CuInS_2$ thin films achieved by spray pyrolysis on glass substrate from solutions containing 0·02 M $CuCl_2{\cdot}2H_2O$, 0·16 M thiourea and 0·08 M $In_2Cl_3{\cdot}5H_2O$.**

Keywords. **$CuInS_2$; doping; structural properties; optical properties; copper compounds; ternary semiconductors; semiconductor epitaxial layers; thin films solar cell; optical constants.**

1. Introduction

The chemical spray pyrolysis (CSP) technique offers an extremely easy way to prepare films with dopants, virtually any element in any proportion by merely adding it in a spray solution. The deposition rate and thickness of the film can easily be controlled for a wide range. It also offers an opportunity to have reactions at low temperatures (100–500°C). These methods can also produce films on substrates that are less robust materials and on large surfaces. The versatile nature of this technique lies in the way various parameters that include effect of precursors, dopants, substrate temperature, *in situ* annealing treatments, solution concentrations and so on can easily be controlled. Various types of metal oxides, metallic spinel oxide, binary and ternary chalcogenides and superconducting oxides can be prepared (Patil 1999).

Ternary chalcopyrite $CuInS_2$ thin films exhibit many excellent physical and chemical properties such as high absorption coefficient in the visible spectral range (Siemer *et al* 2001), high tolerance to the presence of defects (Aksenov and Sato 1992), direct bandgap close to 1·5 eV, the optimum value for the photovoltaic conversion of solar energy (Scheer *et al* 1995), possibility to avoid n- and p-type conductivity (Shay and Wernick 1975) and high chemical stability. In contrast to other ternary semiconductor materials, $CuInS_2$ is nontoxic, low-cost and easy to fabricate by various thin film deposition techniques (Hashimoto *et al* 2005; NcNatt *et al* 2005; Zribi *et al* 2005a, b). For controlling a conduction type and obtaining low resistivity, several impurities doped $CuInS_2$ bulks have been studied. Akaki *et al* (2006) studied the structural, electrical and optical properties of Bi–$CuInS_2$ thin films grown by vacuum evaporation method. Zribi *et al* (2005) investigated the effect of Na doping on the properties of $CuInS_2$ thin films and obtained more interesting results. The incorporation of Fe during crystal growth of $CuInS_2$ by chemical vapour transport was studied by Brandt *et al* (1983) and Ueng and Hwang (1990) and the results of electrical and photoluminescence measurements of P-doped and Zn-doped $CuInS_2$ crystals were reported (Yamamoto and Yoshida 1996; Yamamoto *et al* 2000) who investigated the electronic structures of n-type doped $CuInS_2$ crystals using Zn and Cd species and showed that p-type doping using the group V elements such as N, P and As increases the Madelung energy, which gives rise to instability of ionic charge distribution in p-type doped $CuInS_2$ crystals

(mhsuhail@yahoo.com)

(Abaab *et al* 1999). Enzenhofer *et al* (2006) showed that the open circuit voltage of solar cells based on $CuInS_2$ can be enhanced via controlled doping of small amounts of zinc.

In this paper, we report on structural and optical properties of the Zn-doped $CuInS_2$ thin films as a function of substrate temperature and Zn concentration.

2. Experimental

The spray pyrolysis technique is a simple technology in which an ionic solution—containing the constituent elements of a compound in the form of soluble salts—is sprayed onto overheated substrates using a stream of clean, dry air. The $CuInS_2$ thin films were prepared by spraying an aqueous solution of In_2Cl_3, $CuCl_2$ and thiourea $[(NH_2)_2CS]$ on glass substrate kept at 250, 300 and 350°C.

The atomization of the chemical solution into a spray of fine droplets is effected by the spray nozzle, with the help of compressed air as carrier gas. The spray rate was about 15 cm^3/min through the nozzle which ensures a uniform film thickness. The apparatus used to carry out the chemical spray process consists basically of a device used to atomize the spray solution and some sort of substrate heater. Our set up consists of a reaction chamber foreseen to its lower part with a plate heated by electrical resistance. Standard commercial glass slides ($25 \times 25 \times 1$ mm^3) were used as substrates, which were previously cleaned well using detergent, water and dried prior to the film deposition process.

Substrate temperature is measured with a thermocouple. Above the substrate at variable distances (10–50 cm) the glass-spraying nozzle is fixed. The solution is sprayed (from a reservoir) by means of the carrier gas, incidently to the substrate. The gas (dry air used as a carrier gas) flow rate was 13 ml/min. The spraying time varied between 10 and 20 s for one layer, and the layer number between 1 and 5. The heater was a cylindrical stainless steel block furnace electrically controlled to an accuracy of ±2 °C. The substrate temperature was varied, while other spray parameters were kept constant. The thickness of the film was 400 nm and established by micro weighting or spectrophotometrically as described in Nascu and Popescu (2004). The X-ray diffraction (XRD) patterns of the films were recorded with a JEOL 60 PA X-ray diffractometer operating with a 0·15418 nm monochromatized Cu–K_α radiation at 40 kV and 30 mA with Ni filter. Transmission and absorption spectra of the prepared samples were measured by normal incidence of light using a double beam UV-3101 PC Scanning Shimadzu spectrophotometer, in the wavelength range 400–1000 nm, using a blank substrate as the reference position.

3. Results and discussion

3.1 *Structure of $CuInS_2$ thin films*

Figure 1 shows X-ray diffraction patterns of undoped $CuInS_2$ thin films which are deposited on glass substrates at substrate temperatures 250, 300, 350°C and substrate temperature, 350°C annealed in air to 200°C for 2·5 h. No XRD peaks corresponding to any phase of crystalline CIS were found when the films were sprayed onto substrates at temperatures lower than 250°C. XRD spectra reveal that all obtained films sprayed at substrate temperatures equal to 250°C or higher are polycrystalline with chalcopyrite structure (JCPDS File No. 047–1372) with a preferred orientation at $2\theta = 27{\cdot}9°$ assigned to the (112) reflection of $CuInS_2$ phase. CIS films prepared show a chalcopyrite structure with present significant differences in their crystalline structure for both temperatures and temperature annealed to 200°C for 2·5 h.

The grain size along the (112) peak can be evaluated by using the Debye Scherrer relation (NcNatt *et al* 2005):

$$L = 0{\cdot}9\,\lambda / \cos(\theta_0)\,\Delta(2\theta)\,, \tag{1}$$

where 2θ is the half intensity width of the peak and θ_0 the Bragg angle.

The FWHM values of the (112) diffraction peak decrease when the substrate temperature rises from 250 to 350°C indicating that the crystallite size is bigger for films sprayed at 350°C. The increase in grain size is due to recrystallization processes.

Although this phenomenon was observed in several samples sprayed under the same conditions, this work focuses on the conditions that make possible the synthesis of crystalline CIS films.

We note also some additional diffraction peaks at different Bragg angles which can be associated to binary compounds In_2S_3, CuS and Cu_2S crystal and these phases were not investigated in detail. This result agreed with Sahal *et al* (2009).

It is clear to state the important role of temperature in the crystallization of films. The pattern of the film displayed diffraction peaks at 2θ values of approximately 16°, 16·75°, 20·73°, 23·42° and 31·63° which corresponds to (002), (101), (242), (200), (220) and (116) planes, respectively. It may be noted that a secondary phase with peaks assigned to (222), (400) and (312) planes appears which is attributed to the Cu_2S, CuS and In_2S_3 material. In addition, we note that an increase in substrate temperatures leads to an improvement in the crystallinity of the films (Ezugwu *et al* 2009, 2010).

3.2 *Structure of $CuInS_2$ thin films doped with zinc*

Figure 2 shows results of our XRD measurements of non-doped and doped $CuInS_2$ thin films with Zn concentration. It is found that the zinc concentration has great effects on the formation of polycrystalline $CuInS_2$. All diagrams present a peak at $2\theta = 27{\cdot}9°$ assigned to the (112) reflection of $CuInS_2$ phase and there is an improvement in the growth of all the samples containing Zn. It is also observed that the intensity of the (112) peak decreases obviously with increasing zinc concentrations, which probably may be due to increase of the disorder component.

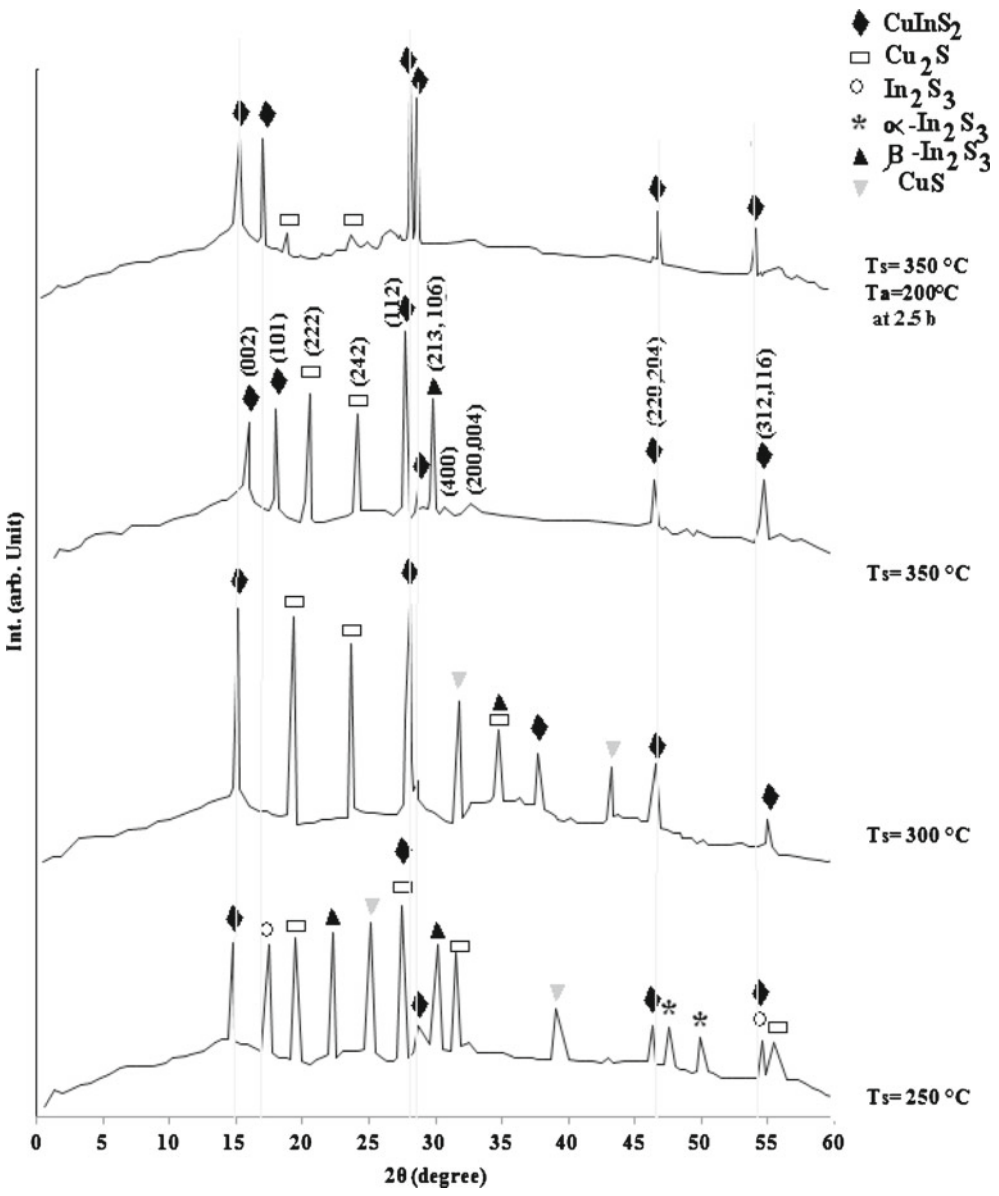

Figure 1. X-ray diffraction patterns of $CuInS_2$ films at different substrate temperatures.

However, we can note a few peaks with lower intensities identified as Cu_2Zn+Cu_4In, CuS, Cu_2S and ZnS phases. The presence of the phases is, in general, attributed to a sum of internal origins obeying the thermodynamics of solid solutions, to defect chemistry and the thermal gradient which plays an important role (Kanzari *et al* 1997). Indeed, additional copper phase is mainly attributed to the higher mobility of Cu^+ and its migration toward the surface layers (Scheer *et al* 1995).

We can note the overlap of zinc in most sites because of the similarity between the electronic-copper and zinc and the appearance of peaks at other locations and a private compound ZnS and shift some peaks which show the entry ions, zinc, to the crystal structure of the compound $CuInS_2$. This is consistent with what is reported by Schorr and his group (Schorr *et al* 2009).

The shortfall in the atoms of sulfur as a result of a link zinc-sulfur led to a surplus in the atoms of indium and copper, which resulted in formation of alloys, Cu_4In and Cu_9In_4, as shown in figure 2.

It has been established by Ueng and Hwang (1990) that in studying the defect structure of zinc-doped $CuInS_2$, we have to consider the basic defect states that would be formed by zinc in $CuInS_2$ crystals. They show that the incorporation of zinc in $CuInS_2$ crystals can occur in three different ways, exclusively occupying the copper site to make a donor, occupying the sulfur site to make an acceptor and occupying the interstitial site to make a donor, and the donor ZnCu and Zn_i would be compensated by the acceptor ZnS. Consequently, it is probable that zinc in our case occupies sulfur site to make an acceptor which can explain the origin of the *p*-type conductivity (Aksay and Altıokka 2007).

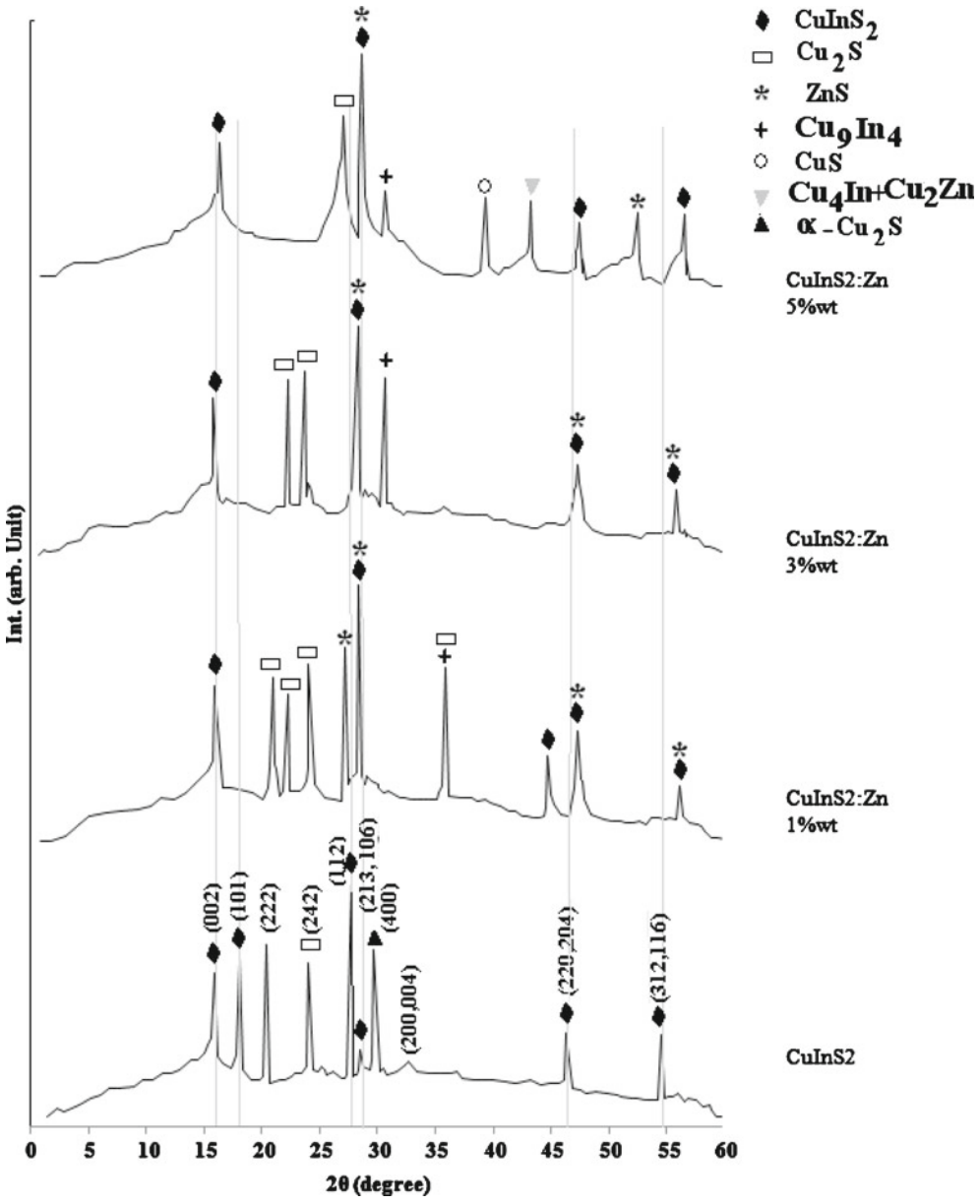

Figure 2. X-ray diffraction patterns of undoped and doped films with Zn.

3.3 *Optical properties*

3.3a *Absorption coefficient and optical bandgaps*: All the transmission spectra show interference pattern with moderate sharp fall of transmittance at the band edge, which is an indication of good crystallinity. The transmission of 1, 3 and 5 Zn % molecular weight doped $CuInS_2$ films are higher than that of the non-doped ones. This indicates that an increase in Zn doping content from a critical Zn % molecular weight value has great effect on the transmission properties.

Therefore, for lower Zn concentrations there is an improvement in crystallinity through occupying the sulfur site by zinc and $CuInS_2$ structure is not affected. Consequently, there is an improvement in transmission in near infrared spectral range and probably the sulfur vacancy sites (samples undoped) increase the absorption. It is clear that the transmission in the near infrared region decreases from 70% to 35% for the higher Zn-incorporation. We consider that the introduced Zn with high amount compensates the sulfur vacancy sites after what the excess Zn atoms present an undesirable effect by decreasing the transmission in the near infrared spectral region. Although the detailed mechanism to explain zinc effect in the decrease of transmission is not clear yet (Ben Rabeh *et al* 2009).

The absorption coefficient (α) has been determined as a function of wavelength from measured reflectance, R and transmittance, T, using the following equation (Tauc *et al* 1966; Milovzorov *et al* 2001)

$$\alpha = 1/d \ \ln\left[(1-R)^2/T\right], \tag{2}$$

where d is the thickness of thin film, R and T the reflection and transmission, respectively.

Figure 3 shows optical absorption coefficient, α, as a function of wavelength for $CuInS_2$ thin films prepared at different substrate temperatures. Higher absorption coefficient is seen at higher substrate temperature.

From figure 4 we can see the values of absorption coefficient (α) increased when the film is annealed in air to 200°C for 2·5 h.

Figure 5 shows absorption coefficient vs wavelength for the undoped and doped $CuInS_2$ thin films with 0 to 5 Zn% molecular weight. It can be seen that all the films have relatively high absorption coefficients. Figure 5 clearly shows an improvement in the optical performance of $CuInS_2$ films doped with 1 Zn % molecular weight with a sharp fall of the absorption at the band edge compared to that of the un-doped or doped with other Zn content. This result is very important because we know that the spectral dependence of absorption coefficient affects the solar conversion efficiency (Mott and Davis 1970).

In the high absorption region close to the beginning of band-to-band optical transmission, the absorption is characterized by the following relation (Fagan and Fritzsche 1970; Sedeek and Fadel 1993).

$$\alpha h\nu = A\left(h\nu - E_{\text{opt}}\right)^r, \tag{3}$$

where A is a constant, E_{opt} the optical gap and r an integer number which characterizes the transition process. The usual method for determining the values of E_{opt} involves plotting a graph of $(\alpha h\nu)^r$ vs $h\nu$.

An appropriate value of (r) is used to linearize the graph, the value of E_{opt} is given by the intercept on the $h\nu$ axis and the constant A can be determined from the slope. The best fit was found to be $r = 1/2$ which indicates that direct photon transition is involved.

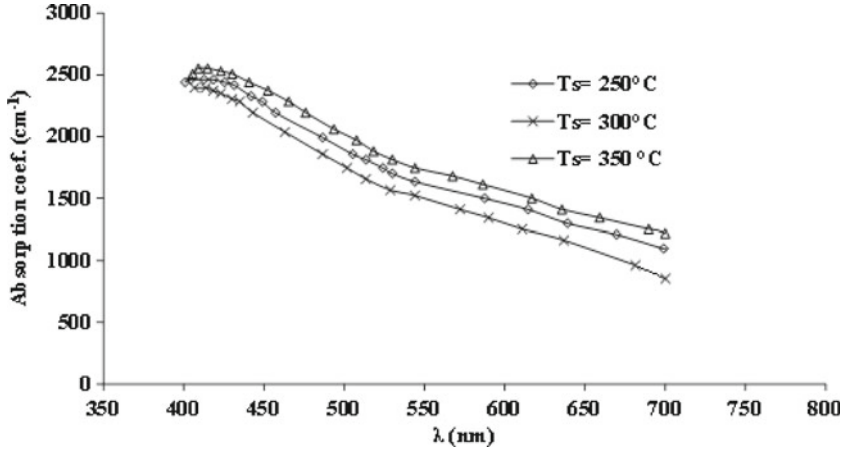

Figure 3. Optical absorption coefficients as a function of wavelength for $CuInS_2$ thin films prepared at different substrate temperatures.

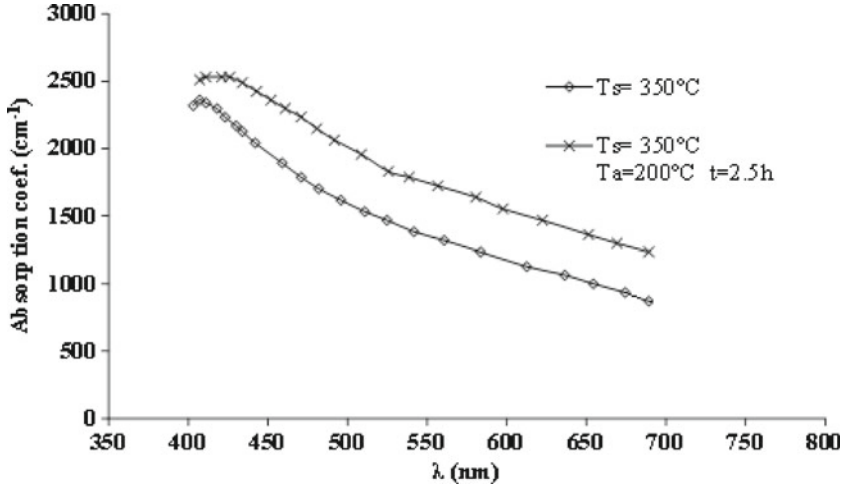

Figure 4. Values of absorption coefficient (α) for film annealed in air to 200°C for 2·5 h.

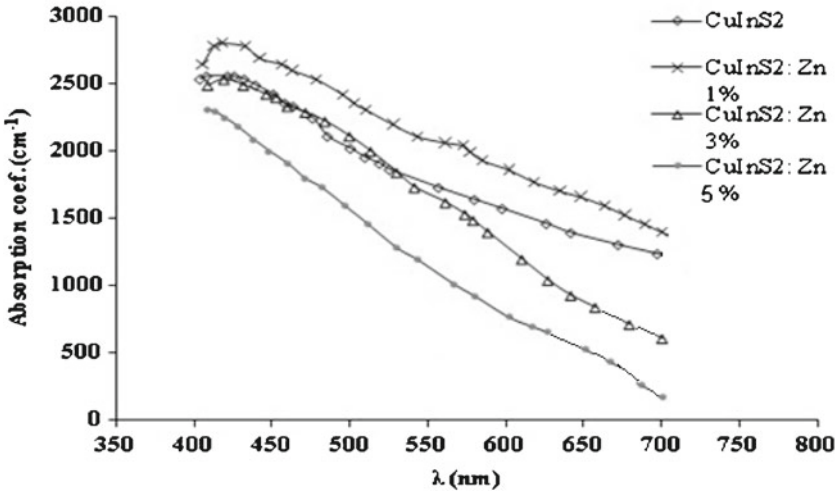

Figure 5. Absorption coefficient vs wavelength for doped $CuInS_2$ thin films with (0–5) Zn % molecular weight.

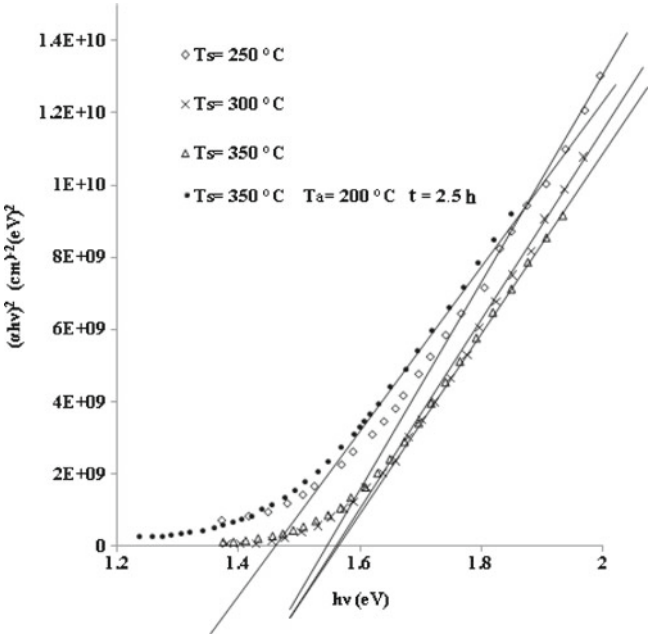

Figure 6. Plot of $(\alpha h\nu)^2$ against photon energy as a function of different T_s.

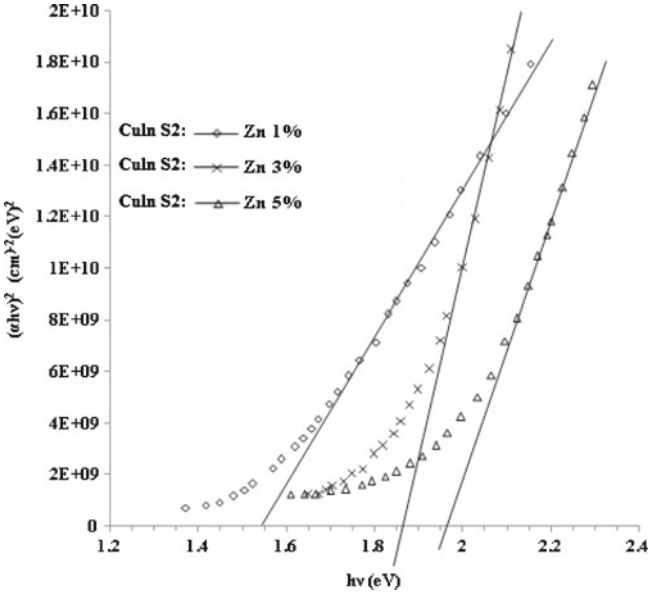

Figure 7. Plot of $(\alpha h\nu)^2$ against photon energy as a function of Zn doped films.

Figure 6 shows a plot of $(\alpha h\nu)^2$ against the photon energy $h\nu$. The bandgap of the films is determined by the extrapolation of the curves. Its value in the films sprayed at ratios of 1 : 1 : 4 is around 1·55 eV at 350°C, which is more than the 1·53 eV energy gap value reported in the literature for $CuInS_2$ (Shay and Wernick 1975).

It is now well established that $CuInS_2$ is a direct gap semiconductor (Tell *et al* 1971; Onnagawa and Miyashita 1985; Nishikawa *et al* 1995), with the band extrema located at the centre of the Brillouin.

The direct bandgap energy stabilizes between 1·55 eV and 1·95 eV with increasing film zinc concentration as shown in figure 7. We attribute this difference to the presence of an amorphous component and possibly the structural defects, since it cannot be excluded that the polycrystallinity of the films influences the optical absorption behaviour and thus also the gap energy derived from the spectra. Also the amount of disorder in the material probably plays an important role in the optical bandgap, since XRD analysis indicated that for the higher Zn % molecular weight a deterioration of the structural properties was observed which give rise to defect states and thus induce smearing of absorption edge (Mott and Davis 1971).

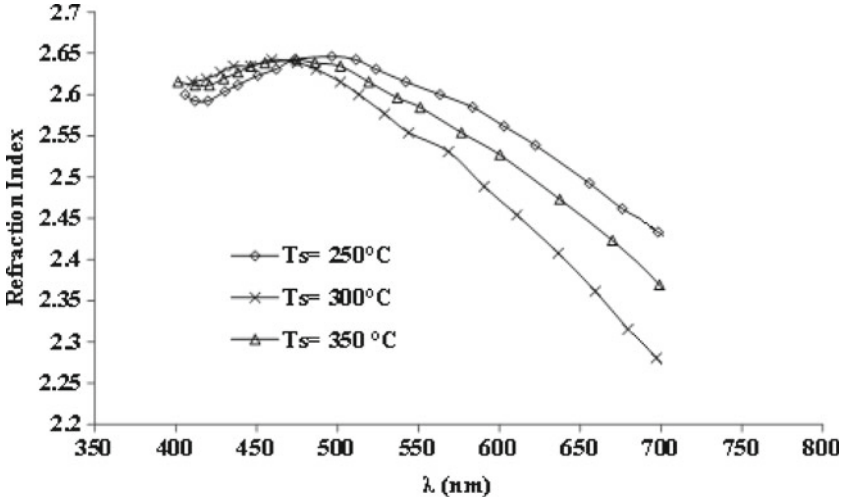

Figure 8. Refractive index of $CuInS_2$ films prepared at different substrate temperatures.

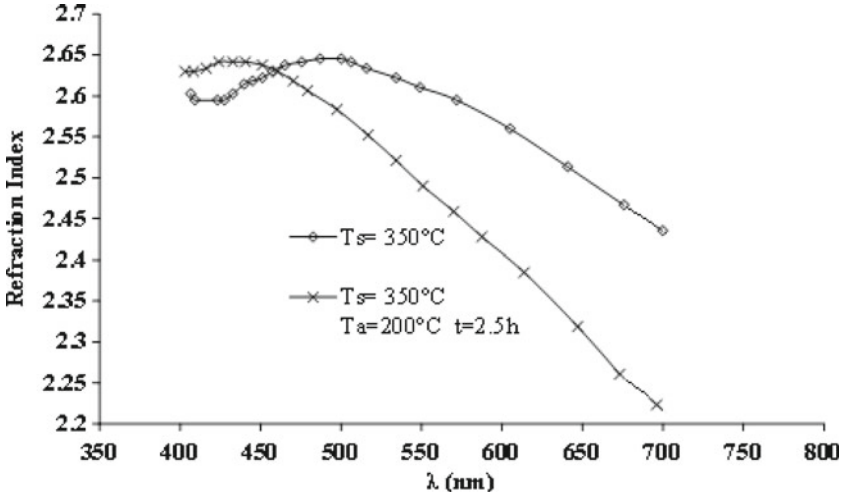

Figure 9. Refractive index of $CuInS_2$ films prepared at $T_s = 350\,°C$ and annealing to 200°C for 2·5 h.

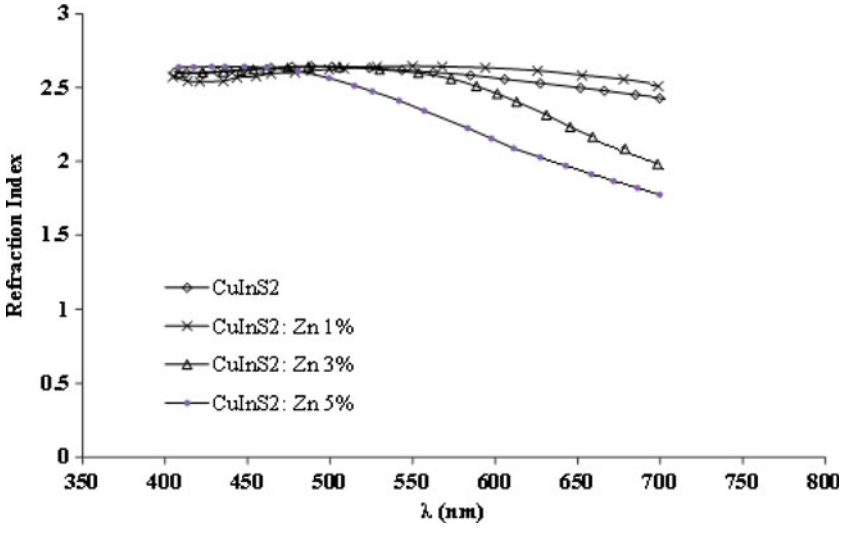

Figure 10. Refractive index of $CuInS_2$ thin films doped with zinc ratios (0–5) wt%.

3.3b *Refractive index*: The refractive index was calculated using the following equation (Heavens 1950).

$$n = \left[4R/(R-1)^2 - K^2\right]^{1/2} - (R+1)/(R-1). \quad (4)$$

We observed from figure 8 that the values of the refractive index of the prepared films are close together in the wavelength between 475 and 375 nm. The values of n at a wavelength of 550 nm were 2·61, 2·54 and 2·58 at a substrate temperature of 250, 300 and 350°C, respectively.

When the films were prepared at a substrate temperature of 350°C and annealed to 200°C for a period of 2·5 h, it was observed that the values of the refractive index (n) was greater than that deposited at $T_s = 350$°C (see figure 9) which had access to the wavelength of 460 nm which reflected the situation with the note to increase the difference between them at greater wavelengths. The value of (n) at the wavelength of 550 nm was 2·492 as in figure 9.

Figure 10 shows refractive index of $CuInS_2$ thin films doped with zinc ratios (1, 3, 5 wt%). We note that the increase in doping decreased the value of refractive index, especially in the region 475–700 nm. The values of (n) at a wavelength of 550 nm were 2·37, 2·6 and 2·615, respectively according to the percentage of doping.

3.3c *Dielectric constant*: The real and imaginary part of dielectric can be calculated from the following two equations (Kanzari *et al* 1997):

$$\varepsilon_1 = n^2 - k^2, \quad (5)$$

$$\varepsilon_2 = 2nk. \quad (6)$$

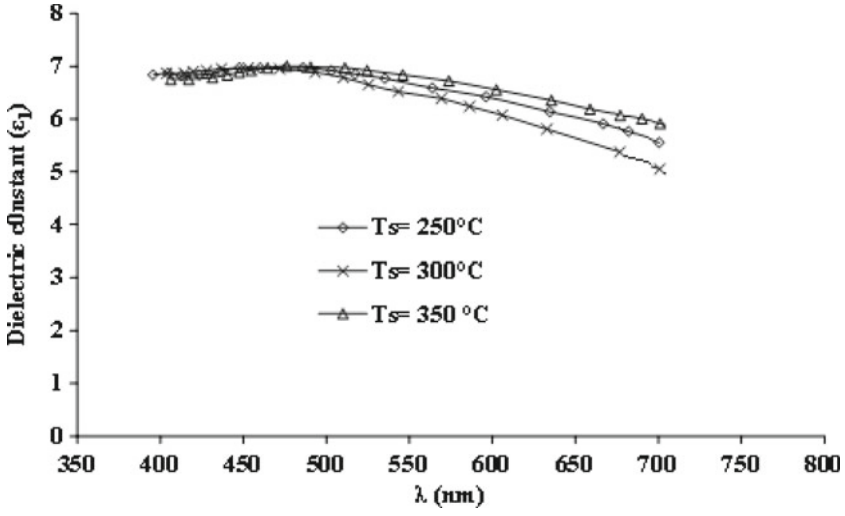

Figure 11. Values of (ε_1) as a function of wavelength for $CuInS_2$ thin films deposited at different T_s.

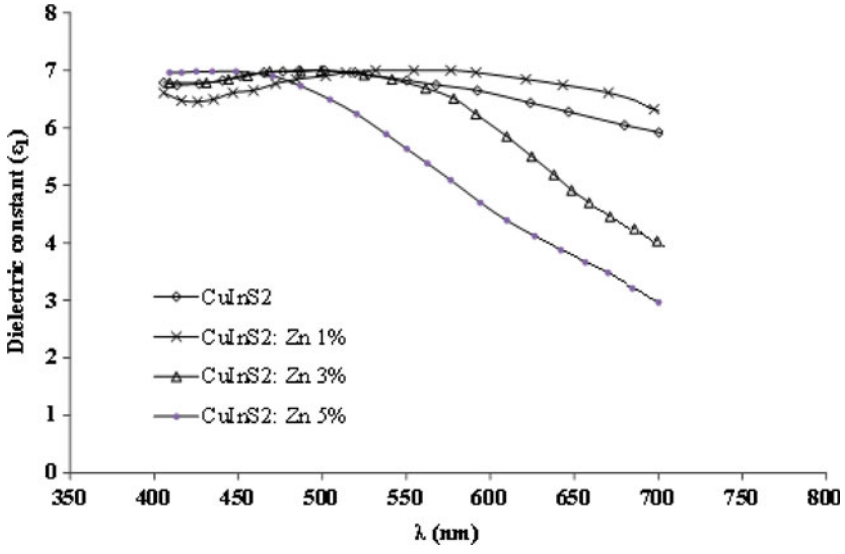

Figure 12. Value of ε_1 as a function of wavelength at different dopings.

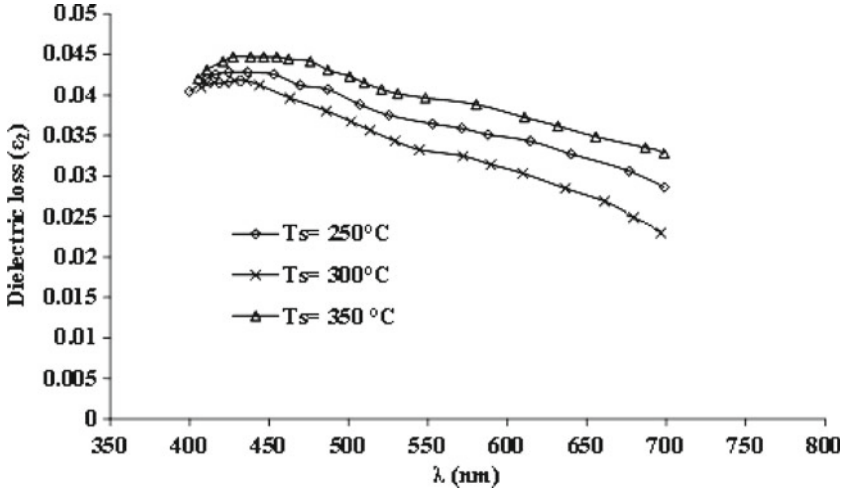

Figure 13. Values of ε_2 as a function of wavelength at different substrate temperatures.

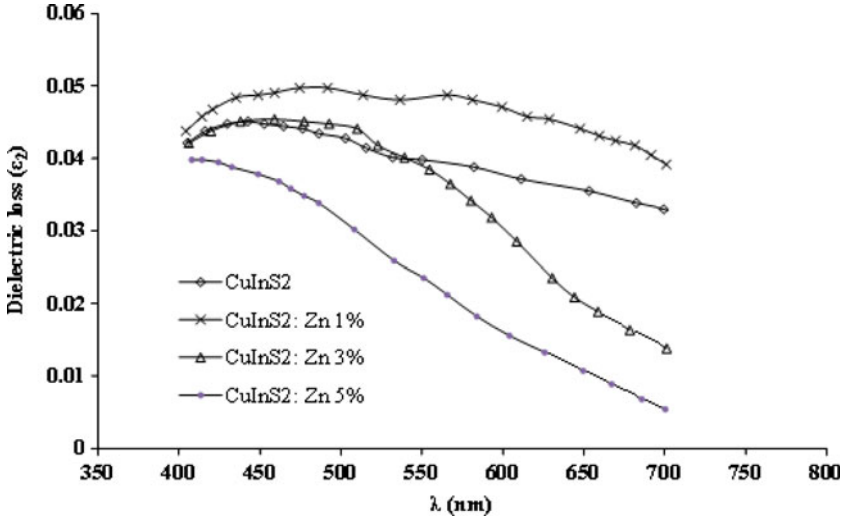

Figure 14. Values of ε_2 as a function of wavelength at different dopings.

Figure 11 shows change in the real part of dielectric constant (ε_1) as a function of wavelength for $CuInS_2$ thin films deposited at different substrate temperatures. We found that the values of ε_1 at a wavelength of 550 nm were 6·49, 6·68, 6·81 at $T_s = 300$, 250 and 350°C, respectively.

When $CuInS_2$ thin films doped with zinc (1, 3 and 5 wt%), we can see from figure 12 that the values of ε_1 decreases in the region of visible wavelength with the increased rate of doping. The values of ε_1 at a wavelength of 550 nm depended on the rates of doping (1, 3, 5) at values of 6·99, 6·775 and 5·85, respectively. From figure 13 we can see the relation between the values of imaginary part of dielectric constant, ε_2 and wavelength. The values of ε_2 decreased when the substrate temperature increased from 250–300°C, but increased when increasing the temperature to 350°C and the values of ε_2 of these films at a wavelength of 550 nm with substrate temperatures basis (300, 250, 350)°C were (3·32, 3·75 and 4·35)10^{-2}, respectively.

From figure 14, the values of ε_2 decreases with increasing doping and the values at the wavelength of 550 nm were (4·525, 3·875 and 2·31)10^{-2} with rates of doping (1, 3, 5) %, respectively.

4. Conclusions

Studies reported here show that it is possible to deposit CIS films using spray pyrolysis technique in ambient atmosphere using compressed air as carrier gas. Sprayed CIS films exhibit a chalcopyrite structure. Structural, chemical composition and optical properties of sprayed films depend on the fabrication conditions, in particular, on the substrate temperature and the Cu/In ratio in the starting solution. It was found that the uniformity, growth rate and adhesion of the films depend strongly on the substrate temperature, spray rate and

solution concentration. The bandgap of about 1·55 eV is in good agreement with the 1·53 eV energy values of CIS single crystal. The effect of Zn doping on the structural and optical properties of $CuInS_2$ thin films has been investigated. It was shown that Zn incorporation is possible and the control of Zn content is an important parameter to obtain Zn-doped $CuInS_2$ layers with high transmission. Moreover, up to 2 at % Zn the transmission decreases which indicates that an increase in doping content deteriorates the transmission properties. The absorption coefficients deduced from optical measurements are $>10^3$ cm^{-1} in the range, 400 nm. The direct bandgap energy increased from 1·467 to 1·95 eV with increasing Zn % molecular weight. We attributed the higher values compared to that corresponding to the evaporated $CuInS_2$ thin films to the structural defects. The Zn-doped $CuInS_2$ thin films exhibit P-type conductivity.

References

Abaab M, Kanzari M, Rezig B and Brunel M 1999 *Solar Energ. Mater. Solar C.* **59** 299

Akaki Y, Matsuo H and Yoshino K 2006 *Phys. Status Solidi (c)* **8** 2597

Aksay S and Altıokka B 2007 *Phys. Status Solidi (c)* **4** 585

Aksenov I and Sato K 1992 *J. Appl. Phys.* **31** 2352

Ben Rabeh M, Kanzari M and Rezig B 2007 *Thin Solid Films* **515** 5943

Ben Rabeh M, Kanzari M and Rezig B 2009 *Acta Physica Polonica* **A115** 699

Brandt G, Ranber A and Schneider J 1983 *Solid State Commun.* **12** 481

Enzenhofer T, Unold T, Scheer R and Schock H W 2006 *Phys. Status Solidi* **A203** 2624

Ezugwu S C, Ezema F I, Osuji R U, Asogwa P U, Ekwealor A B C and Ezekoye B A 2009 *Optoelectron. Adv. Mater.-Rapid Commun.* **3** 141

Ezugwu S C, Ezema F I and Asogwa P U 2010 *Chalcogenide Lett.* **7** 369

Fagan E A and Fritzsche H 1970 *J. Non-Cryst. Solids* **2** 80

Hashimoto T, Merdes S, Takayama N, Nakayama H, Nakanishi H, Chichibou S F and Ando S 2005 *20th European photovoltaic solar energy conference, Proceedings of the international conference, Barcelona* (eds) W Palz *et al*, p. 1926

Heavens O S 1950 *Optical properties of thin solid films* (London: Butterworths)

Kanzari M, Abaab M, Rezig B and Brunel M 1997 *Mater. Res. Bull.* **32** 1009

Milovzorov D E, Ali A M, Inokuma T, Kurata Y, Suzuki T and Hasegawa S 2001 *Thin Solid Films* **382** 47

Mott N F and Davis E A 1970 *Philos. Mag.* **22** 903

Mott N F and Davis E A 1971 *Electronic processes in non-crystalline materials* (Oxford: Clarendon Press)

Nascu Horea Iustin and Popescu Violeta 2004 *Leonardo Electronic J. Practices Technol.* 22

NcNatt J S, Dickman J E, Hepp A F, Kelly, Jin M H C and Banger K K 2005 *Conference record of the 31st IEEE photovoltaic specialists conference, Lake Buena vista, Florida*, p. 375

Nishikawa N N, Aksenov I, Sinzato T, Sakamoto T and Sato K 1995 *Jpn. J. Appl. Phys.* **34** L975

Onnagawa H and Miyashita K M 1985 *J. Appl. Phys.* **23** 965

Patil P S 1999 *Mater. Chem. Phys.* **59** 185

Sahal M, Marí B and Mollar M 2009 *Thin Solid Films* **517** 2202

Scheer R, Diesner K and Lewerenz H J 1995 *Thin Solid Films* **168** 130

Schorr S, Tovar M, Hoebler H J and Schock H W 2009 *Thin Solid Films* **517** 2508

Sedeek K and Fadel M 1993 *Thin Solid Films* **229** 223

Shay J L and Wernick J H 1975 *Ternary chalcopyrite semiconductors, growth, electronic properties and applications* (Oxford, New York: Pergamon Press)

Siemer K, Klaer J, Luck I, Bruns J, Klenk R and Braunig D 2001 *Sol. Energ. Mater. Sol. C.* **67** 159

Tauc J, Grigorovici R and Vancu A 1966 *Phys. Status Solidi* **15** 627

Tell B, Shay J I and Kasper H M 1971 *Phys. Rev.* **B4** 2463

Ueng H Y and Hwang H L 1990 *J. Phys. Chem. Solids* **51** 11

Yamamoto T and Yoshida H K 1996 *Jpn. J. Appl. Phys.* **35** L1562

Yamamoto T, Luck V and Scheer R 2000 *Appl. Surf. Sci.* **159–160** 350

Zribi M, Kanzari M and Rezig B 2005a *20th European photovoltaic solar energy conference, Proceedings of the international conference, Barcelona* (eds.) W Palz *et al*, p. 1890

Zribi M, Kanzari M and Rezig B 2005b *Jpn. J. Appl. Phys.* **29** 203